

Chapter 5A) Formulation Development: Omiganan Nano-lipid Constructs

Dermal Delivery of Protein/Peptide Based Antimicrobial to Treat Secondary Infection in Psoriasis and Eczema

5A.1 Introduction

The objective of our present investigation was to develop and characterize novel nano-lipid constructs (NLC) of Omiganan for dermal delivery. These NPs can control the release of the therapeutic agent and ensure delivery in the desired manner and have been widely reported in the literature [1-3]. Several molecules (hydrophobic/hydrophilic) have been encapsulated in the NLCs by the melt-emulsification method followed by high-pressure homogenization (HPH). Hence, this method was selected to prepare Omiganan loaded NLCs out of several available methods [4-7]. A systematic Quality-by-design (QbD) approach employing statistical design of experiments was utilized to exhaustively evaluate the impact of material attributes and process parameters on the critical formulation attributes [8].

5A.2 Materials and Instruments

5A.2.1 Materials

Table 5A.1 List of materials

Materials & Reagents	Manufacturers
Omiganan	S-Biochem, Kerala, India (Custom synthesis)
Methanol (A.R. & HPLC Grade)	Spectrochem Pvt. Ltd., Mumbai
Miglyol- 840	Gattefosse, Mumbai
Precirol-ATO-5	Gattefosse, Mumbai
Tween 80	MP Biomedicals Pvt. Ltd., Mumbai
PEG 400	MP Biomedicals Pvt. Ltd., Mumbai
Distilled water	Prepared In-house

5A.2.2 Instruments

Table 5A.2 List of instruments

Equipment	Manufacturer
Digital Weighing Balance	Shimadzu, Japan
RP-HPLC with UV Detector (gradient)	Agilent OpenLab CDS EZChrom, India
Vortex mixer	Spinix, Japan
Magnetic stirrer	Remi equipments Pvt Ltd., India
pH meter	Lab India Pvt. Ltd, Mumbai

Bath Sonicator	Remi equipments Pvt. Ltd, India
Filtration assembly	Durga scientific Pvt. Ltd., Baroda
Centrifuge	Remi equipments Pvt. Ltd., India
Distillation assembly	Durga glassware, India
High Pressure Homogenizer	Avestin, India
Particle size analyzer (Nano-ZS)	Malvern Instrument, UK
Scanning electron microscope	EVO-18, Zeiss, Germany

5A.3 Methodology

5A.3.1 Preparation of Omiganan loaded nano-lipid constructs

Omiganan loaded NLCs were prepared by using the melt-emulsification method [4-7]. Briefly, Precirol-ATO-5 and Miglyol- 840 were taken in 6:4 ratios. The aqueous phase was ready by dissolving the Tween 80 and PEG 400 in 5 ml of PBS pH 5.5. Both of these phases were maintained at 75°C, and Omiganan (%1w/w) was transferred into the melted lipid matrix, subsequently the addition of the aqueous phase to the lipid phase drop by drop under the continuous stirring at 700 rpm using a magnetic stirrer at room temperature to get a homogeneous emulsion. The resultant NLC particles were then subjected to HPH (10000 psi * 10 cycles) for size reduction. Subsequently, this NLC dispersion was centrifuged at 18,000 rpm for 30 min at 4 °C to separate the free Omiganan and NLCs.

5A.3.2 QbD approach for the formulation development

Before developing any formulation, there is a strong need to identify formulation variables, process variables, and environmental variables expected to affect the product characteristics. Ishikawa diagram (Fig. 5A.1) was used to determine all the probable variables, i.e., formulation, process, and environment variables connected with the development of Omiganan loaded NLCs by melt-emulsification method (Table 5A.3).

Table 5A.3 List of variables mainly affecting Omiganan NLC formulation

Formulation variables	Process variables	Environment variables
Drug (Omiganan)	Mixing of components	Temperature
Concentration of Lipids	The volume of organic phase	
Drug: lipid ratio	Stirring speed	
Smix concentration	Stirring time	
Lipid phase volume	Rate of addition of organic phase	
pH of solution	Bead size	

Quality Target Product Profile (QTPP)

For the development of an accurate, precise, and reproducible manufacturing method as a quality target product profile, the following attributes were considered that will ensure desired product quality in all aspects of QTPP:

- ✓ % Entrapment Efficiency and % drug loading: high
- ✓ Particle Size: 200-300 nm
- ✓ Drug release from nano-lipid constructs: NLT 60% in 6 hr

5A.3.2.1 Optimization of Formulation by Box-Behnken Design (BBD)

Optimization by varying one-variable-at-a-time is an intricate way to examine the effect of variables on an experimental outcome. This tactic measures one variable at a time rather than all at the same time. BBD is used for the optimization of formulation for the following reasons: [9, 10]

- The BBD technique is a 3-level design based on combining two-level factorial designs and incomplete block designs.
- This cubic design is categorized by a set of points lying at the midpoint of each edge and a replicate center point of the multidimensional cube.
- It requires fewer runs than 3-factor, 3-level Full Factorial Design and Central Composite Design (CCD)
- BBD is a spherical design with exceptional predictability within the spherical design space. Additionally, the BBD technique is considered the most appropriate to examine the quadratic response surfaces, mainly when the prediction of response at the extreme level is not the goal of the model.

The selected variable values for BBD i.e., independent variables and dependent variables (response parameters) are shown in Table 5A.4.

Table 5A.4 Selected values of variables for BBD

Variables	Levels (-1, 0, 1)
Independent variables	
A: Lipid concentration (%w/w) (X1)	2,3,4
B: Smix concentration (%w/w) (X2)	5,10,15
C: Homogenization cycles (No.) (X3)	5,10,15
Constant parameters	
Rate of organic phase addition (ml/min)	1 ml/min
The volume of organic solvent (ml)	2 ml
Stirring time (min)	30 min
Stirring speed (rpm)	700 rpm
Homogenization pressure (psi)	10000 psi
Temperature (°c)	25-40°C (room temp.)
Dependent variables (response parameters)	
% Drug entrapment (%) (Y1)	
Particle size (nm) (Y2)	

The selection of critical formulation variables was made according to the results obtained in the preliminary investigation. A BBD design matrix was generated using Stat-Ease Design-Expert Software 13.0. Total 17 experimental runs were obtained from the software. All the batches of Omiganan nano-lipid constructs were prepared according to the design matrix while keeping all other process variables constant. % Drug entrapment and particle size of the formulated Omiganan nano-lipid constructs were taken as response parameters (CQA).

5A.3.2.2 Particle size

The particle size of Omiganan loaded NLCs were determined using Nano-ZS Zetasizer, Malvern Instruments Ltd., UK. Briefly, Omiganan NLC dispersion was diluted 10 times with filtered distilled water and transferred to disposable sizing cuvette/folded capillary cells to measure particle size. It uses the Mie theory of light scattering to calculate the mean diameter of NLCs.

5A.3.2.3 % Drug entrapment

To determine the % drug entrapment, Omiganan NLC dispersion was centrifuged at 18,000 rpm for 30 min at 4 °C. The sedimented NLC fraction was dissolved in water: methanol (2:8) mixture and analyzed by the developed HPLC method (chapter 3). To ensure the mass balance of the drug, the supernatant was also analyzed for the free Omiganan content using the HPLC method at 220 nm. % Drug loading was quantified by using the mass (weight) of the centrifuged pellet of NLCs. Following equations were used to estimate the % drug entrapment and % drug loading: [11]

$$\% \text{ Drug entrapment} = \frac{\text{Amount of entrapped drug}}{\text{Total drug added}} \times 100$$

$$\% \text{ Drug loading} = \frac{\text{Drug loaded (mg)}}{\text{Total weight of NLCs (mg)}} \times 100$$

5A.3.2.4 Preparation of gel for Omiganan and Omiganan nano-lipid constructs

The gel-based formulation was developed and loaded with Omiganan (1% w/v) and optimized Omiganan NLCs (having 1% w/v Omiganan concentration) to improve the viscosity of the formulation for better skin retention. Carbopol 934P, a polyacrylic acid-based gelling agent is extensively used in topical formulations due to its better hydration and wetting properties. Briefly, the weighed quantity of Carbopol 934P (1.2% w/v) was mixed and dispersed in Omiganan NLC dispersion (1% w/v) using an overhead stirrer at 2000 rpm for 1 h. After hydration, the mixture of methylparaben (0.2% w/v) and propylparaben (0.02% w/v) in propylene glycol (4% w/v), was added with continuous stirring. The pH of the formulation was adjusted to ~6.5 by dropwise addition of 10% v/v Sodium hydroxide solution. The detailed formulation composition is showed in Table 5A.5.

Table 5A.5 Formulation components and concentration used in the preparation of Omiganan NLC gel

Formulation components	Concentration
Omiganan/Omiganan NLCs	1% w/v
Carbopol 934P	1.20% w/v
Propylene glycol	4% w/v
Methyl paraben and propyl paraben	0.2 and 0.02 %w/v
Sodium hydroxide solution (10% v/v)	...qs...to pH 6.5

5A.3.3 Characterization of optimized Omiganan NLCs and NLC gel

5A.3.3.1 Zeta potential

The zeta potential of Omiganan NLC dispersion was measured using a Nano-ZS zeta sizer equipped with a 5-mV He-Ne laser. Briefly, Omiganan NLC dispersion was diluted 10 times with filtered distilled water and transferred to disposable folded capillary cells. An average of 30 measurements of each sample was used to get average zeta potential.

5A.3.3.2 Shape and surface morphology

The optimized Omiganan loaded NLCs were examined for scanning electron microscopy (SEM). Briefly, the sample was gold-coated using a sputter coater (Emitech) for 4 min at 10 mA current. After that, sample was attached to the aluminium stubs and then observed using an accelerating voltage of 15.00 kV at different magnifications.

5A.3.3.3 Viscosity of Omiganan gel

The viscosity of free Omiganan gel and Omiganan NLC gel was determined using cone and plate rheometer (Bohlin C-VOR, Malvern Instruments Ltd., UK) at $25\pm1^{\circ}\text{C}$. In brief, 200 mg of the sample was placed on the sample holder. After that, the spindle was lowered and kept for equilibrium for 5 min having a plate width of 20 mm and a cone angle of 4° . Subsequently, the spindle was rotated at a shear rate of 10/s, and viscosity (Pa.S) observed was reported (n=3) [12].

5A.3.3.4 Spreadability of Omiganan gel

The spreadability of free Omiganan gel and Omiganan NLC gel was evaluated by the previously reported method [13]. Briefly, 500 mg of sample was placed on a pre-marked circle with a 1 cm diameter on the glass plate over which a second glass plate was positioned. Subsequently, 500 g weight was applied on the upper glass plate for 5 min, and any change in diameter was reported (n=3).

5A.3.3.5 pH of Omiganan gel

The pH of free Omiganan gel and Omiganan NLC gel was measured using a digital pH meter (Lab India Pvt. Ltd, Mumbai).

5A.3.3.6 Assay of Omiganan gel

The Omiganan content from the free Omiganan gel and Omiganan NLC gel was determined by dissolving the 100 mg of sample in the PBS pH 7.4: methanol mixture (8:2 ratio). The amount of Omiganan was quantified by the developed gradient HPLC method.

5A.4 Results and Discussion

5A.4.1 Preparation and optimization of Omiganan nano-lipid constructs

5A.4.1.1 Establishment of QTPP

The variables linked with the development of Omiganan loaded NLCs by reverse-phase evaporation were identified into Process, Formulation, and Environment. Ishikawa diagram (Fig. 5A.1) was used to demonstrate the variables associated with the development of Omiganan loaded NLCs.

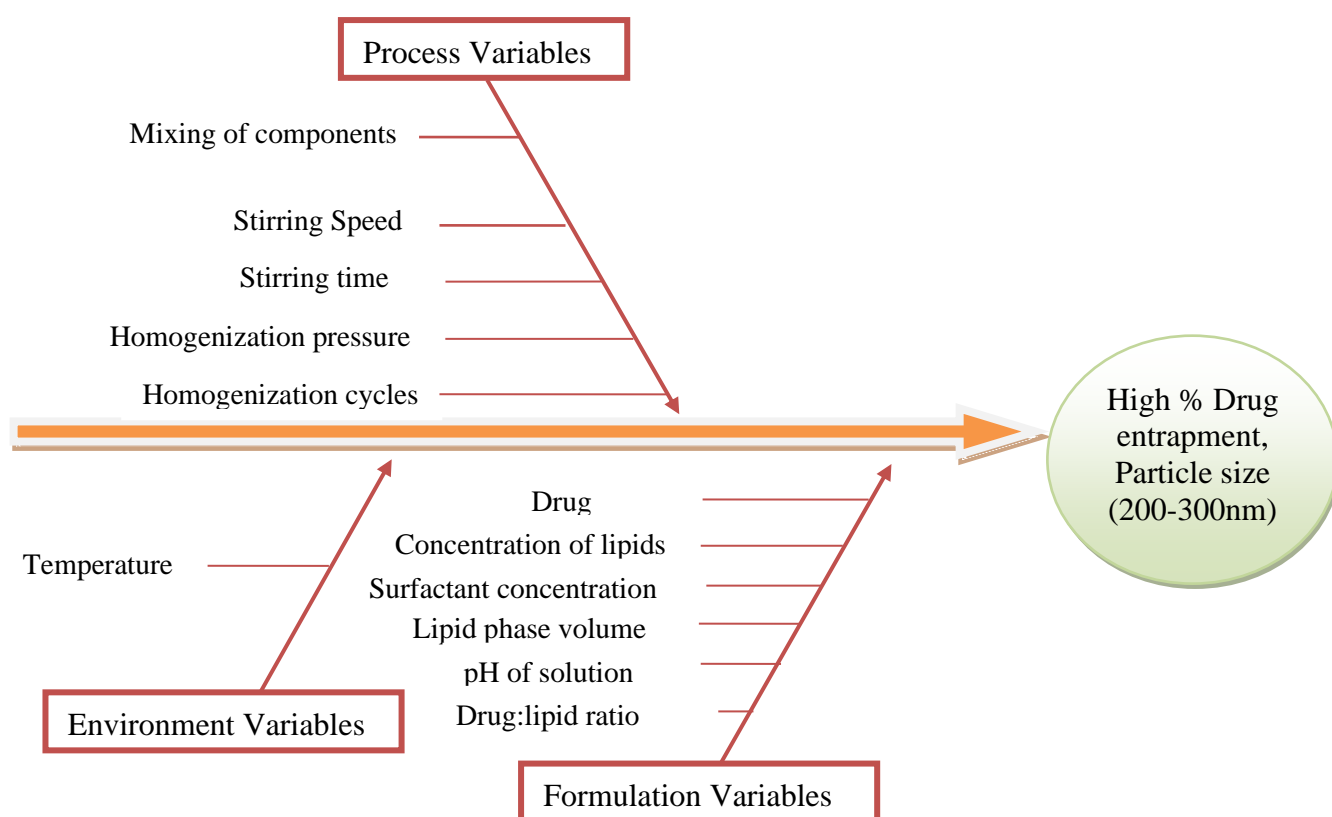


Fig. 5A.1 Ishikawa diagram showing probable variables that may influence CQA

5A.4.1.2 Formulation optimization by Box-Behnken Design

Based on the preliminary investigation, three CMA were identified, and their relationship with CQA was exhaustively investigated using Box-Behnken Design. A randomized matrix of 17 runs was generated by Design-Expert software and presented in Table 5A.6.

Table 5A.6 Randomized BBD design matrix generated by Design-Expert software

Run	Independent variables			Dependent variables (CQA)	
	Lipid concentration (% w/w)	Smix concentration (% w/w)	Homogenization cycles (No.)	% Drug entrapment	Particle size (nm)
1	3	10	10	78.66	112.6
2	3	5	15	72.49	138.2
3	4	10	15	79.09	146.7
4	3	15	5	81.23	153.8
5	3	10	10	80.02	115.4
6	2	10	5	69.91	125.7
7	2	15	10	66.5	120.6
8	2	10	15	63.37	102.9
9	3	5	5	78.64	166.8
10	3	10	10	79.87	117.6
11	3	10	10	79.33	118.3
12	3	15	15	76.24	132.1
13	2	5	10	65.53	117.6
14	4	10	5	83.54	194.2
15	3	10	10	78.12	110.9
16	4	15	10	82.45	160.8
17	4	5	10	81.76	177.4

5A.4.1.3 Effect analysis of critical variables on responses**5A.4.1.3.1 Influence of investigated parameters on % Drug entrapment****A) Statistical Analysis for % Drug entrapment**

The statistical analysis of the design mentioned above is as follows:

Table 5A.7 Statistical analysis of design for % Drug entrapment

Source	Sequential p-value	Lack of Fit p-value	Adjusted R ²	Predicted R ²	
Linear	< 0.0001	0.0088	0.8176	0.7583	
2FI	0.9835	0.0045	0.7665	0.5352	
Quadratic	0.0002	0.2677	0.9773	0.8996	Suggested
Cubic	0.2677		0.9837		Aliased

As shown in Table 5A.7, the best model to fit the experimental results of drug entrapment in nano-lipid constructs is the quadratic model and was chosen for further evaluation.

B) ANOVA Analysis for % Drug entrapment

The ANOVA for % Drug entrapment is given in table 5A.8.

Table 5A.8 ANOVA for Response Surface Quadratic Model for % Drug entrapment

Source	Sum of Squares	df	Mean Square	F-value	p-value	
Model	630.49	9	70.05	77.37	< 0.0001	significant
A-Lipid concentration	473.24	1	473.24	522.68	< 0.0001	
B-Smix concentration	8.00	1	8.00	8.84	0.0207	
C-Homogenization cycles	61.22	1	61.22	67.61	< 0.0001	
AB	0.0196	1	0.0196	0.0216	0.8872	
AC	1.09	1	1.09	1.21	0.3084	
BC	0.3364	1	0.3364	0.3715	0.5614	
A ²	72.73	1	72.73	80.33	< 0.0001	
B ²	4.07	1	4.07	4.50	0.0716	
C ²	4.79	1	4.79	5.29	0.0550	
Residual	6.34	7	0.9054			

Lack of Fit	3.74	3	1.25	1.92	0.2677	Not significant
Pure Error	2.60	4	0.6491			
Cor Total	636.82	16				

The Model F-value of 77.37 implies the model is significant. In this case, A, B, C, A² are significant model terms. The Lack of Fit F-value of 1.92 implies the Lack of Fit is not significant relative to the pure error. The value of ANOVA shows that the effects of factors were significant; hence, the model is significant for % drug entrapment. From ANOVA table 5A.8, we can observe that F value was high for Factor A (522.68) and Factor C (67.61) than Factor B (8.84), it indicates that all the factors affect the % drug entrapment, which can also be observed visually from the surface plots (contour plots and 3D plots). Among the variables affecting % drug entrapment, lipid concentration and homogenization cycles have maximum effect on % drug entrapment. In addition, the actual v/s predicted plot for % drug entrapment shows an R² of 0.9900 which is a good correlation (Fig. 5A.2)

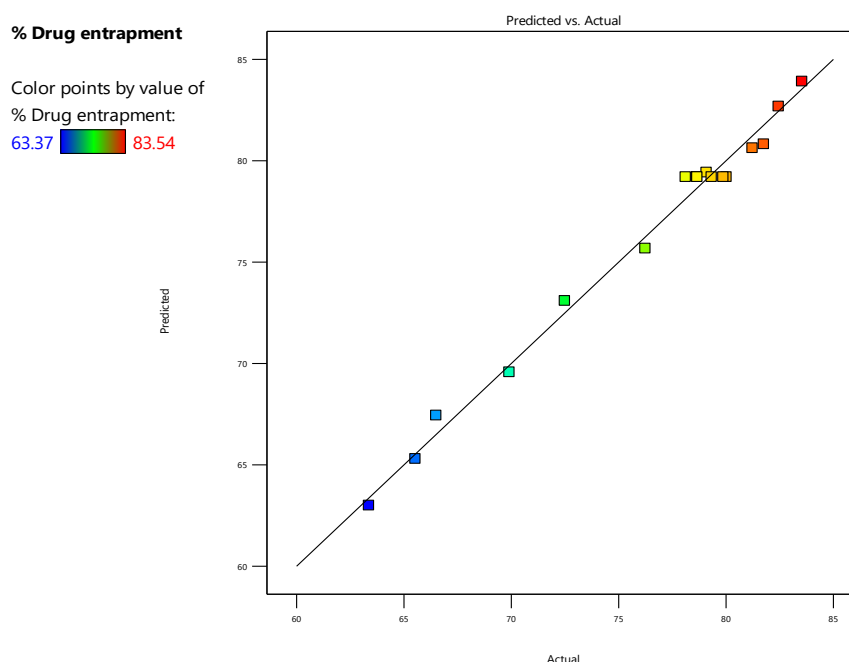


Figure 5A.2 Actual v/s Predicted plot for % Drug entrapment

Table 5A.9 ANOVA study results for % Drug entrapment

Parameters	Results of Response
Std Deviation	0.9515
Mean	76.28
C.V.%	1.25
R-Squared	0.9900
Adjusted R-Squared	0.9773
Predicted R-Squared	0.8996
Adeq. Precision	28.6588

C) Mathematical Model for % Drug entrapment

To examine the effect of various factors on % drug entrapment, contour plots and the 3D plot were referred to along with the value of ANOVA. From Table 5A.8, we can observe that with change in the combination of various levels of factors, the final response, i.e., % drug entrapment confirming the effect of various factors. Looking closely at different factor involved provide us a better understanding of the extent of the impact. The equation talks about the type of effect that is positive or negative.

The final equation in terms of coded factors:

$$\% \text{ Drug entrapment} = 79.2 + 7.69125 * A + 1 * B - 2.76625 * C - 0.07 * AB + 0.5225 * AC + 0.29 * BC - 4.15625 * A^2 - 0.98375 * B^2 - 1.06625 * C^2$$

The final Equation in Terms of Actual Factors

% Drug entrapment	=
+17.92750	
+31.72375	Lipid concentration
+0.913000	Smix concentration
-0.129750	Homogenization cycles
-0.014000	Lipid concentration * Smix concentration
+0.104500	Lipid concentration * Homogenization cycles
+0.011600	Smix concentration * Homogenization cycles

-4.15625	Lipid concentration ²
-0.039350	Smix concentration ²
-0.042650	Homogenization cycles ²

Additionally, from the above equation, we can observe that all the factors affected % drug entrapment to some extent. For example, an increase in lipid concentration increases % drug entrapment. There was an increase in % drug entrapment with an increase in lipid concentration, which may be owing to the partitioning of Omiganan into the lipidic phase [14, 15]. While the decrease in % drug entrapment was found with an increase in homogenization cycles to some extent. Whereas, increase in % drug entrapment was observed with an increase in surfactant concentration to some extent. Surfactant may favour the stabilization of particles and encapsulation of drug into the nanoparticles [16]. Fig. 5A.3-5A.8 demonstrates the effects of independent variables on the % drug entrapment. The red area shows the maximum % drug entrapment, and the blue zone represents the area with the lowest % drug entrapment.

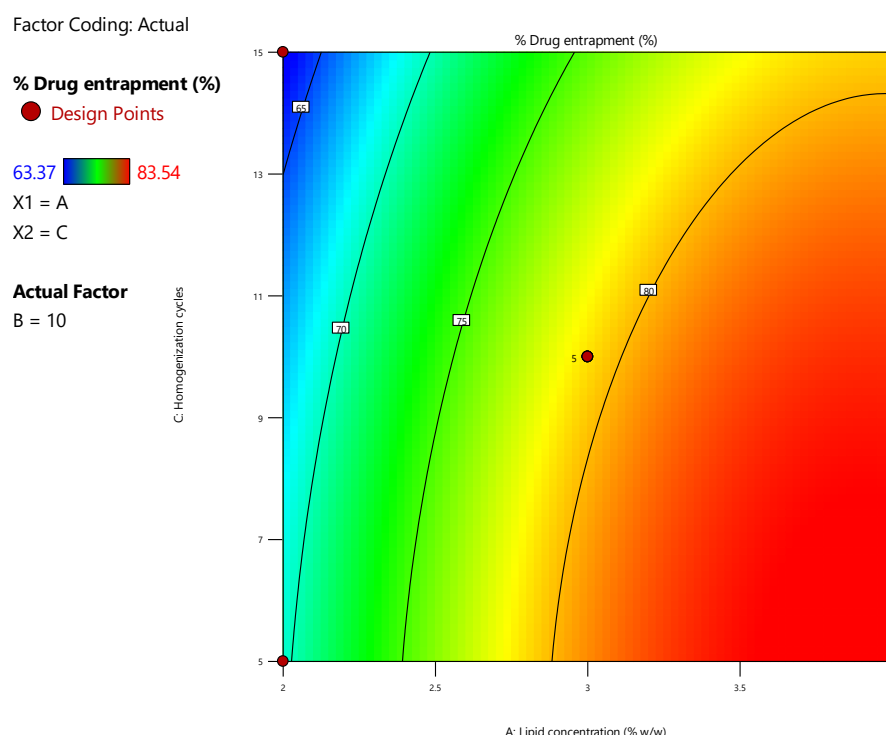


Figure 5A.3 Contour plot (2D) showing the combined effect of lipid concentration and homogenization cycles on % drug entrapment

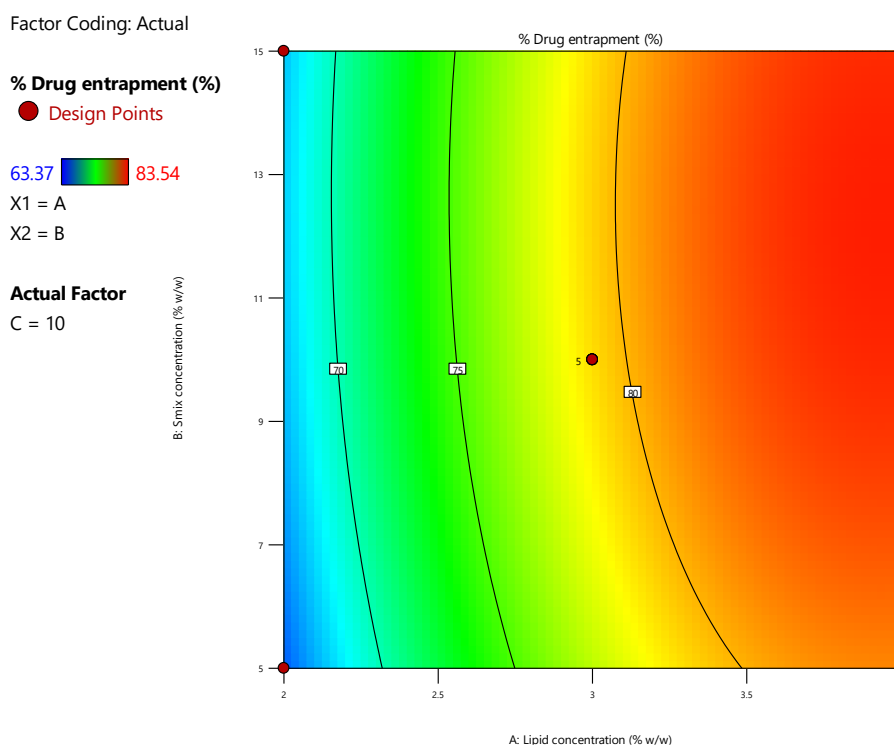


Figure 5A.4 Contour plot (2D) showing the combined effect of lipid concentration and Smix concentration on % drug entrapment

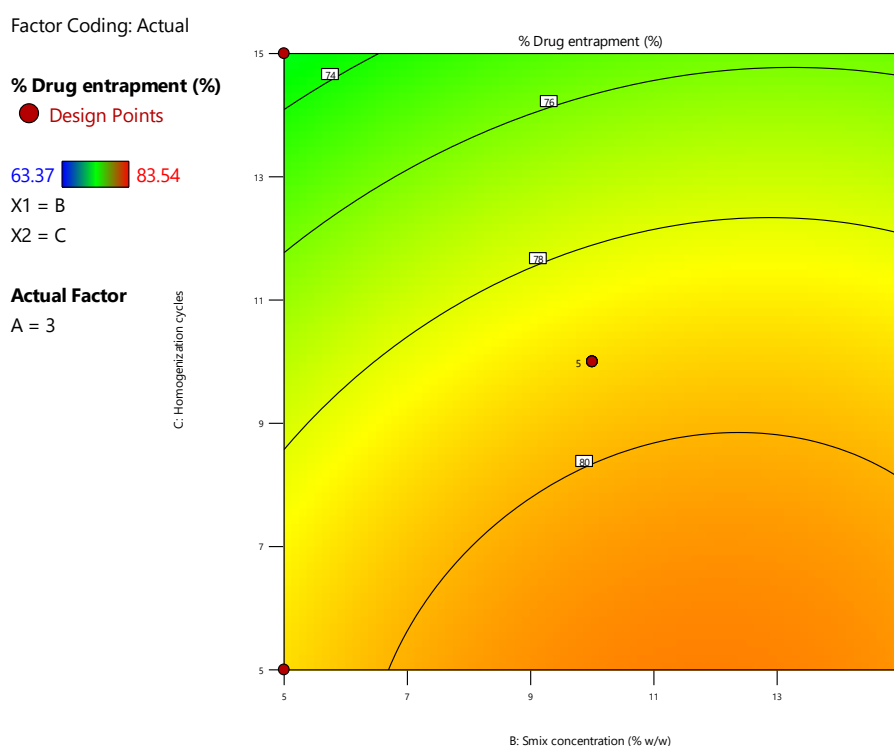


Figure 5A.5 Contour plot (2D) showing the combined effect of Smix concentration and Homogenization cycles on % drug entrapment

Factor Coding: Actual

% Drug entrapment (%)

Design Points:

● Above Surface

○ Below Surface

63.37  83.54

X1 = A

X2 = C

Actual Factor

B = 10

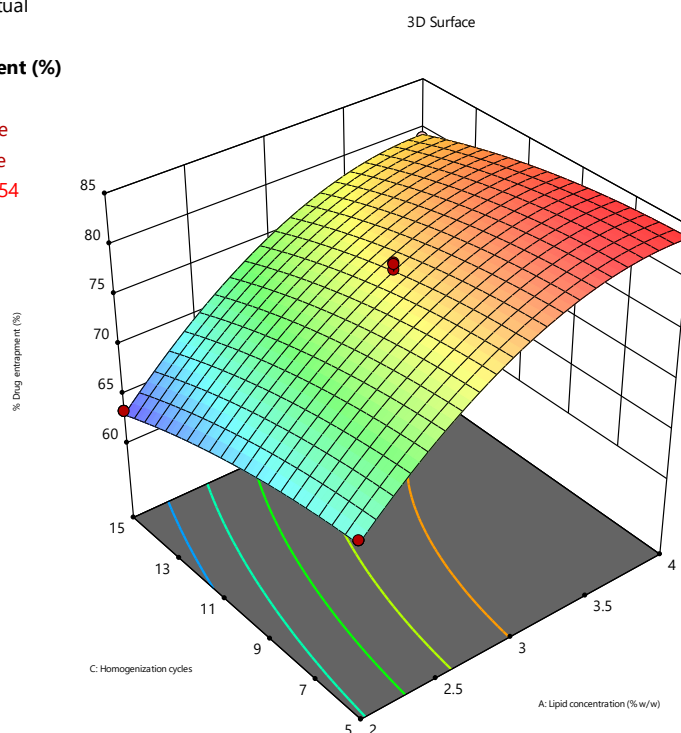


Figure 5A.6 Response surface (3D) showing the combined effect of lipid concentration and Homogenization cycles on % drug entrapment

Factor Coding: Actual

% Drug entrapment (%)

Design Points:

● Above Surface

○ Below Surface

63.37  83.54

X1 = A

X2 = B

Actual Factor

C = 10

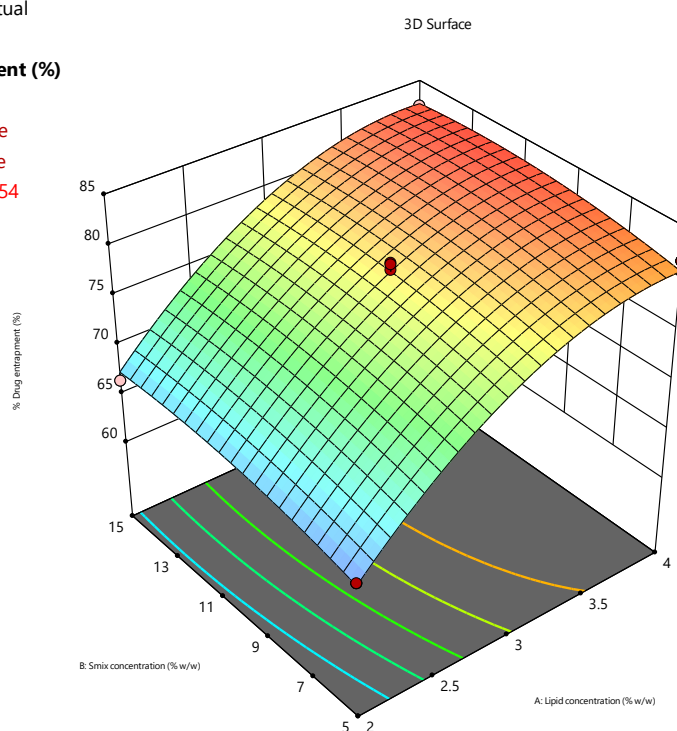


Figure 5A.7 Response surface (3D) showing the combined effect of lipid concentration and Smix concentration on % drug entrapment

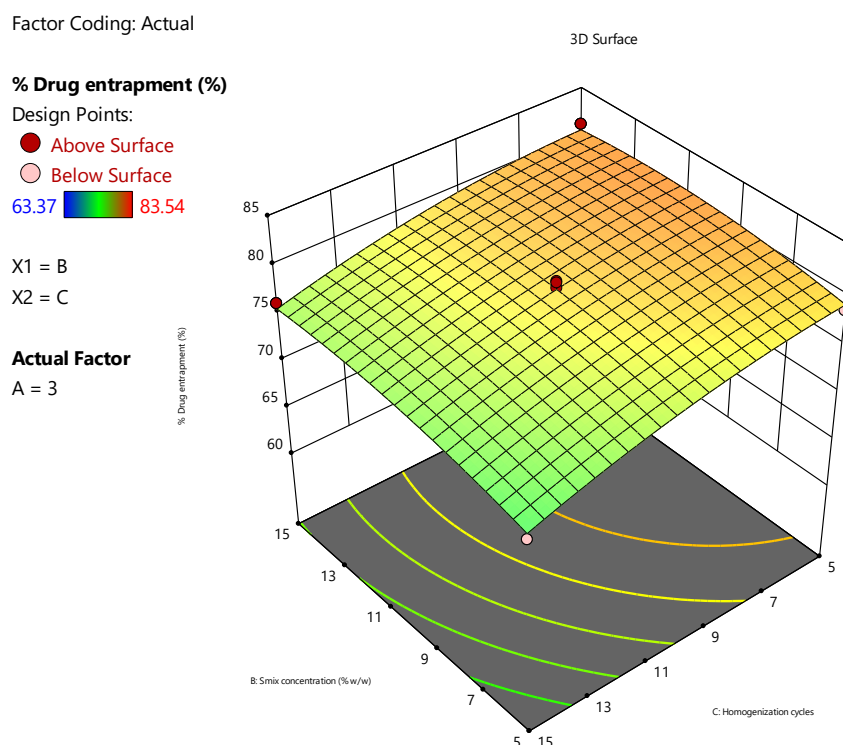


Figure 5A.8 Response surface (3D) showing the combined effect of Smix concentration and Homogenization cycles on % drug entrapment

5A.4.1.3.2 Influence of investigated parameters on Particle size

A) Statistical Analysis for Particle size

The statistical analysis of the design mentioned above is as follows:

Table 5A.10 Statistical analysis of design for Particle size

Source	Sequential p-value	Lack of Fit p-value	Adjusted R ²	Predicted R ²	
Linear	0.0016	0.0015	0.6067	0.5257	
2FI	0.8505	0.0009	0.5262	0.2872	
Quadratic	< 0.0001	0.2084	0.9768	0.8900	Suggested
Cubic	0.2084		0.9855		Aliased

As shown in Table 5A.10, the best model to fit the experimental results of Particle size in nano-lipid constructs is the quadratic model and was chosen for further evaluation.

B) ANOVA Analysis for Particle size

The ANOVA for Particle size is given in Table 5A.11.

Table 5A.11 ANOVA for Response Surface Quadratic Model for Particle size

Source	Sum of Squares	df	Mean Square	F-value	p-value	
Model	11034.39	9	1226.04	75.91	< 0.0001	significant
A-Lipid concentration	5633.91	1	5633.91	348.80	< 0.0001	
B-Smix concentration	133.66	1	133.66	8.28	0.0238	
C-Homogenization cycles	1818.05	1	1818.05	112.56	< 0.0001	
AB	96.04	1	96.04	5.95	0.0449	
AC	152.52	1	152.52	9.44	0.0180	
BC	11.90	1	11.90	0.7369	0.4191	
A ²	595.75	1	595.75	36.88	0.0005	
B ²	1252.17	1	1252.17	77.52	< 0.0001	
C ²	1014.19	1	1014.19	62.79	< 0.0001	
Residual	113.06	7	16.15			
Lack of Fit	72.69	3	24.23	2.40	0.2084	Not significant
Pure Error	40.37	4	10.09			
Cor Total	11147.45	16				

The Model F-value of 75.91 implies the model is significant. In this case, A, B, C, AB, AC, A², B², C² are significant model terms. The Lack of Fit F-value of 2.40 implies the Lack of Fit is not significant relative to the pure error.

The value of ANOVA shows that the effects of factors were significant; hence, the model is significant for % Particle size. From ANOVA Table 5A.11, we can observe that F value was high for Factor A (348.80) and Factor C (112.56) than Factor B (8.28), it indicates that all the factors affect the particle size to some extent which can also be observed visually from the surface plots (contour plots and 3D plots). Among the variables affecting particle size, lipid concentration and Homogenization cycles have maximum effect on particle size. The increase in particle size was observed with increase in lipid concentration. The viscosity of the dispersed

phase (melted lipidic phase) will increase with an increase in lipid concentration and thus increase the size of the dispersion, which may be the possible reason for the increase in the particle size. While, the increase in homogenization cycles reduces particle size as previously reported [17, 18]. In addition, the actual v/s predicted plot for Particle size shows an R^2 of 0.9899 which is a good correlation (Fig. 5A.9).

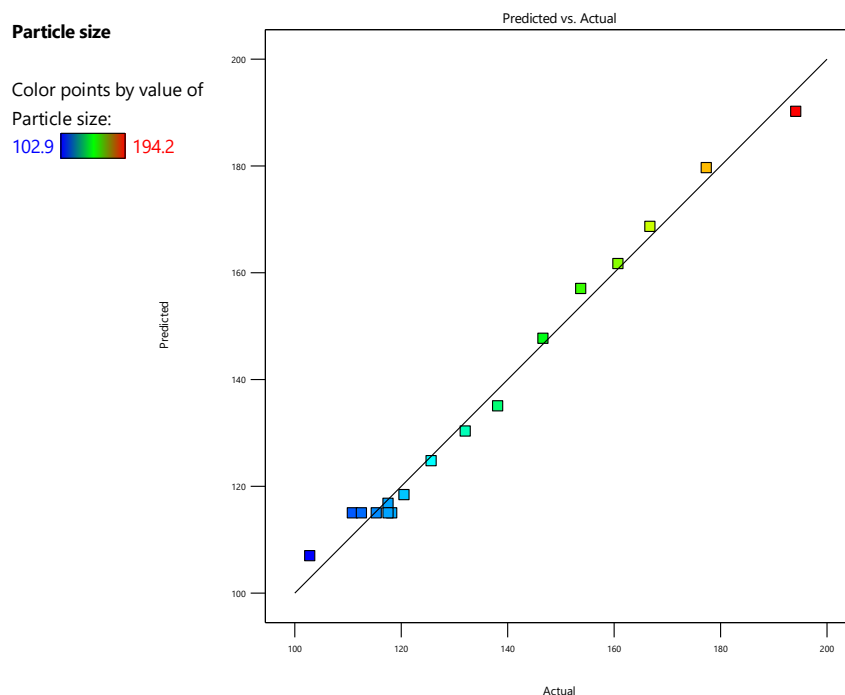


Figure 5A.9 Actual v/s Predicted plot for Particle size

Table 5A.12 ANOVA study results for Particle size

Parameters	Results of Response
Std. Deviation	4.02
Mean	135.98
C.V. %	2.96
R-Squared	0.9899
Adjusted R-Squared	0.9768
Predicted R-Squared	0.8900
Adeq. Precision	27.00

C) Mathematical Model for Particle Size

To evaluate the effect of various factors on Particle size, contour plots and 3D plots were referred to along with the value of ANOVA. From Table 5A.11, we can

observe that with change in the combination of various levels of factors, the final response, i.e., Particle size confirming the effect of various factors. Looking closely at different factor involved provide us a better understanding of the extent of the impact. The equation talks about the type of effect that is positive or negative.

The final equation in terms of coded factors:

$$\text{Particle size} = 114.96 + 26.5375 * A - 4.0875 * B - 15.075 * C - 4.9 * AB - 6.175 * AC + 1.725 * BC + 11.895 * A^2 + 17.245 * B^2 + 15.52 * C^2$$

The final equation in terms of Actual factors:

Particle size	=
+252.23750	
+22.68250	Lipid concentration
-12.36350	Smix concentration
-12.41600	Homogenization cycles
-0.980000	Lipid concentration * Smix concentration
-1.23500	Lipid concentration * Homogenization cycles
+0.069000	Smix concentration * Homogenization cycles
+11.89500	Lipid concentration ²
+0.689800	Smix concentration ²
+0.620800	Homogenization cycles ²

Additionally, from the above equation, we can observe that all the factors affected particle size to some extent. Moreover, lipid concentration and homogenization cycles have maximum effect on the particle size. The increase in particle size was observed with increased lipid concentration. The viscosity of the dispersed phase (melted lipidic phase) will increase with an increase in lipid concentration and thus increase the size of the dispersion, which may be the possible reason for the increase in the particle size. While, the increase in homogenization cycles reduces particle size as previously reported [19, 20]. Fig. 5A.10-5A.15 demonstrates the effects of independent variables on particle size. The red area shows maximum Particle size, and blue zone represents the area with the lowest particle size.

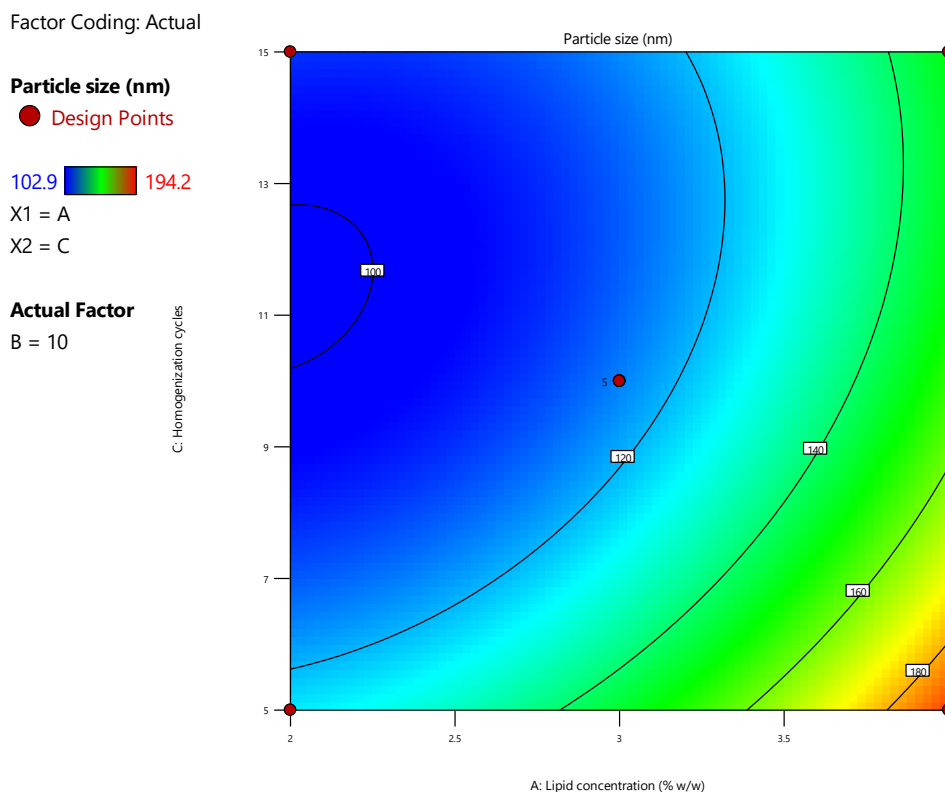


Figure 5A.10 Contour plot (2D) showing the combined effect of lipid concentration and Homogenization cycles on Particle size

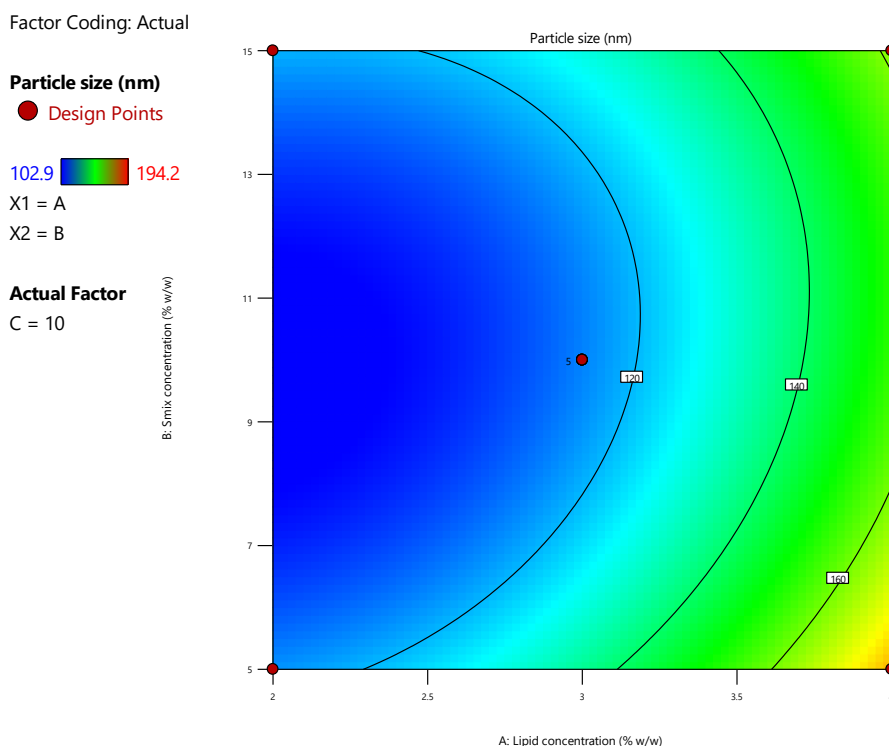


Figure 5A.11 Contour plot (2D) showing the combined effect of lipid concentration and Smix concentration on Particle size

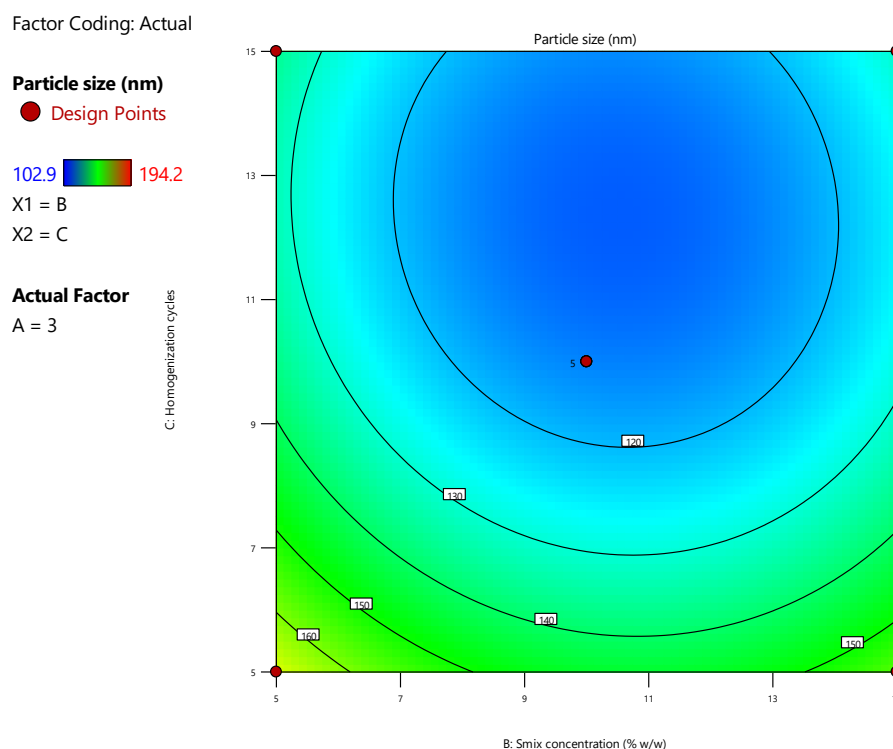


Figure 5A.12 Contour plot (2D) showing the combined effect of Smix concentration and Homogenization cycles on Particle size

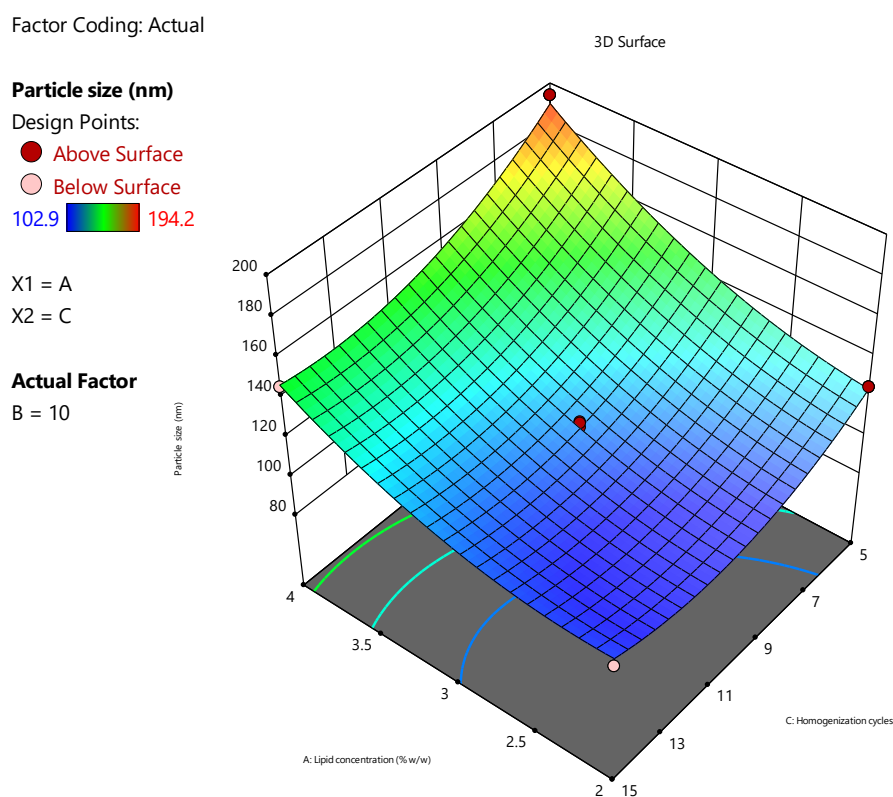


Figure 5A.13 Response surface (3D) showing the combined effect of lipid concentration and Homogenization cycles on Particle size

Factor Coding: Actual

Particle size (nm)

Design Points:

● Above Surface

○ Below Surface

102.9 194.2

X1 = A

X2 = B

Actual Factor

C = 10

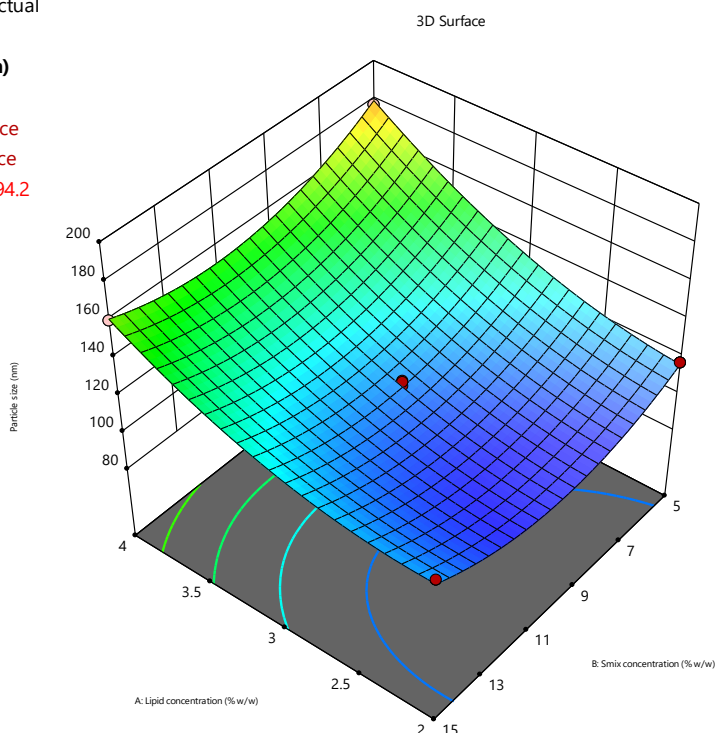


Figure 5A.14 Response surface (3D) showing the combined effect of lipid concentration and Smix concentration on Particle size

Factor Coding: Actual

Particle size (nm)

Design Points:

● Above Surface

○ Below Surface

102.9 194.2

X1 = B

X2 = C

Actual Factor

A = 3

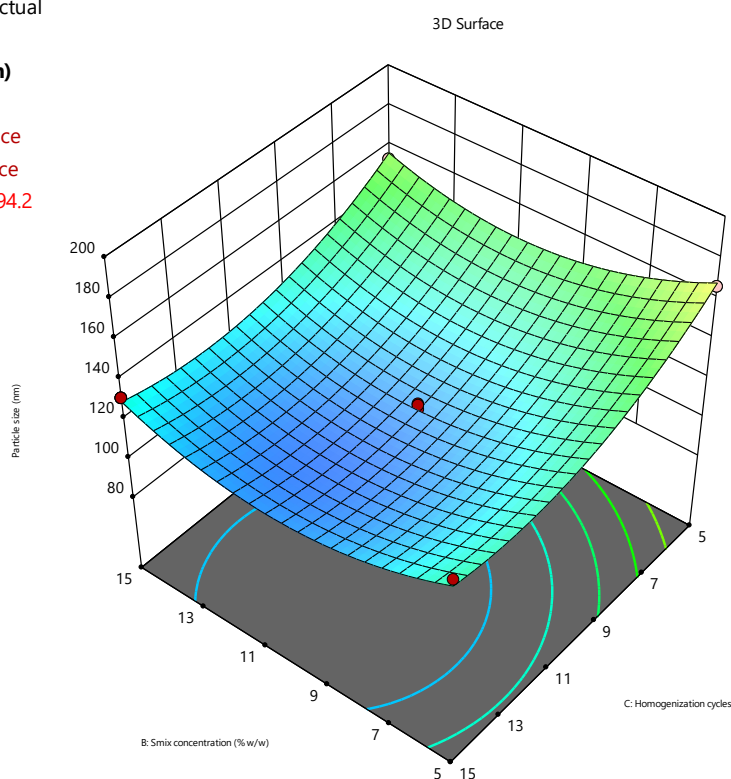


Figure 5A.15 Response surface (3D) showing the combined effect of Smix concentration and Homogenization cycles on Particle size

5A.4.1.3.3 Optimization using Desirability plot

A desirability plot gives the optimum value of variables to get desired responses. A desirability plot was generated (Fig. 5A.16) using Design Expert 13.0. Parameters for the desirability batch are shown in Table 5A.13 and the evaluation of the desirability batch in Table 5A.14.

Table 5A.13 Variables for desirability plot and goals for response

Name	Goal	Lower Limit	Upper Limit
A: Lipid concentration (% w/w)	In range	2	4
B: Smix concentration (% w/w)	In range	5	15
C: Homogenization cycles (No.)	In range	5	15
% Drug entrapment (%)	Maximize	63.37	83.54
Particle size (nm)	Minimize	102.9	194.2

Factor Coding: Actual

All Responses

● Design Points

0.000 1.000

X1 = A

X2 = B

Actual Factor

C = 10

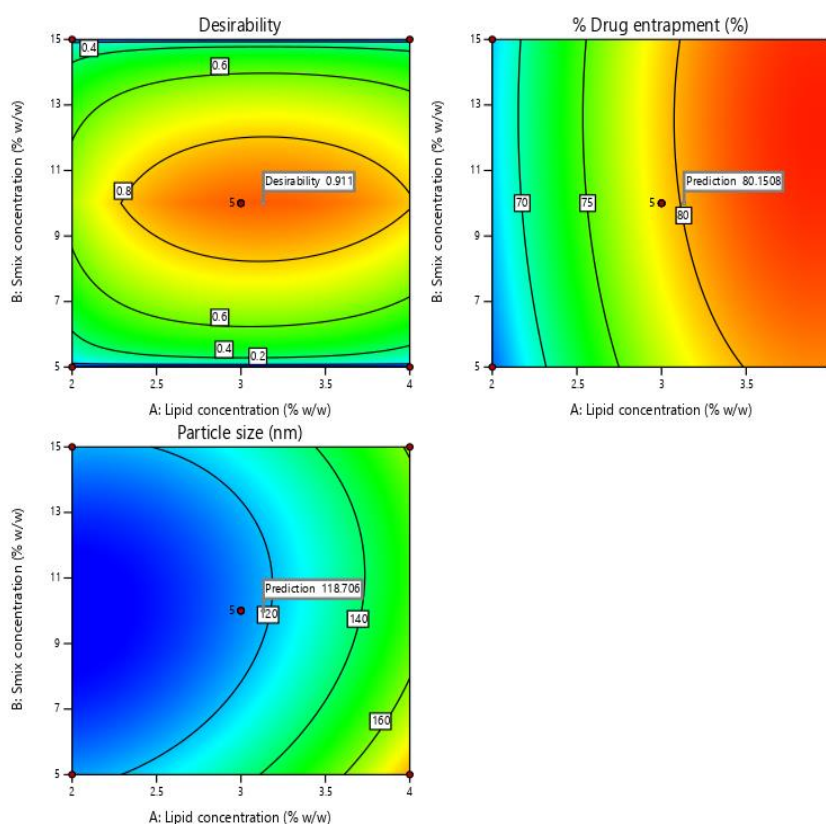


Figure 5A.16 Desirability plot

Table 5A.14 Desirability Plot for Optimization solution for Omiganan nano-lipid constructs

Exp. Run	Lipid concentration (%w/w)	Smix concentration (%w/w)	Homogenization cycles (No.)	% Drug entrapment	Particle size (nm)	Desirability
1	3.133	10	10	80.151	118.71	0.911

Table 5A.15 Results of Evaluation of desirability batch

Response	Experimental value	Predicted value	Residual Difference
% Drug entrapment	79.20	80.151	1.11
Particle size (nm)	115.7	118.71	3.01

The obtained results demonstrate the suitability of the predicted desirability plot of the optimized NLC formulation.

5A.4.1.3.4 Establishment of Design Space

ICH Q8 (2008) defines “Design Space” as a “multidimensional combination and interaction input variables and process parameters that have been established to provide assurance of quality.” The composite desirability function based on the set constraints was used to determine the conditions that would result in an optimal formulation design.

5A.4.1.3.5 Overlay Plot for predicted design space

The experimental design was used for numerous responses: % Drug entrapment and particle size. Overlay plot (Fig. 5A.17) can be obtained by superimposing contour plots of both responses, which displays possible response values in the factor space. The region highlighted in yellow is where a slight variation in the critical variables won't affect the final response and the response will be in the desired range. Areas that do not fit the optimization criteria are shaded gray, while design space is accepted colored yellow. Fig. 5A.17 shows an overlay plot based on the desirability criteria.

Factor Coding: Actual

Overlay Plot

% Drug entrapment

Particle size

● Design Points

X1 = A

X2 = B

Actual Factor

C = 10

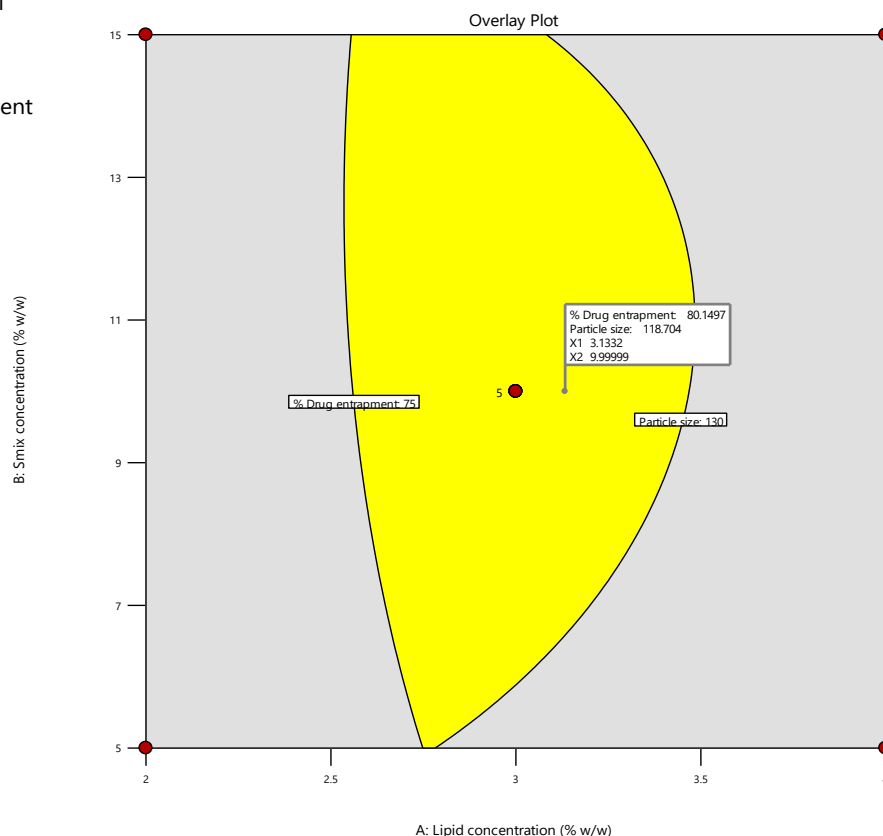


Figure 5A.17 Overlay plot

Table 5A.16 Composition of optimized batch of Omiganan NLCs and gel

Formulation components	Concentration
Omiganan/Omiganan NLCs	1% w/v
Lipid concentration	3.133 % w/w
Smix concentration	10 % w/w
Homogenization cycles	1000 psi * 10 cycles
Carbopol 934P	1.20% w/v
Propylene glycol	4% w/v
Methyl paraben	0.2 % w/v
Propyl paraben	and 0.02 % w/v
Sodium hydroxide solution (10% v/v)	...qs...to pH 6.5

5A.4.2 Characterization of optimized Omiganan nano-lipid constructs and Omiganan NLC gel

5A.4.2.1 Zeta potential

The zeta potential graph of optimized Omiganan nano-lipid constructs (Fig. 5A.18) showed a net negative charge of nano-lipid constructs with a Z-avg value of -16.1 mV. The charge was found sufficient enough to keep the particles dispersed via repulsive forces.

5A.4.2.2 Shape and surface morphology

Scanning electron microscopy of optimized Omiganan nano-lipid constructs was performed, and the image is represented as Fig. 5A.19. The image showed the spherical shape of nano-lipid constructs. The size of nano-lipid constructs seen in the image was found in line with the results of particle size data obtained from the Malvern zeta sizer (Fig. 5A.20).

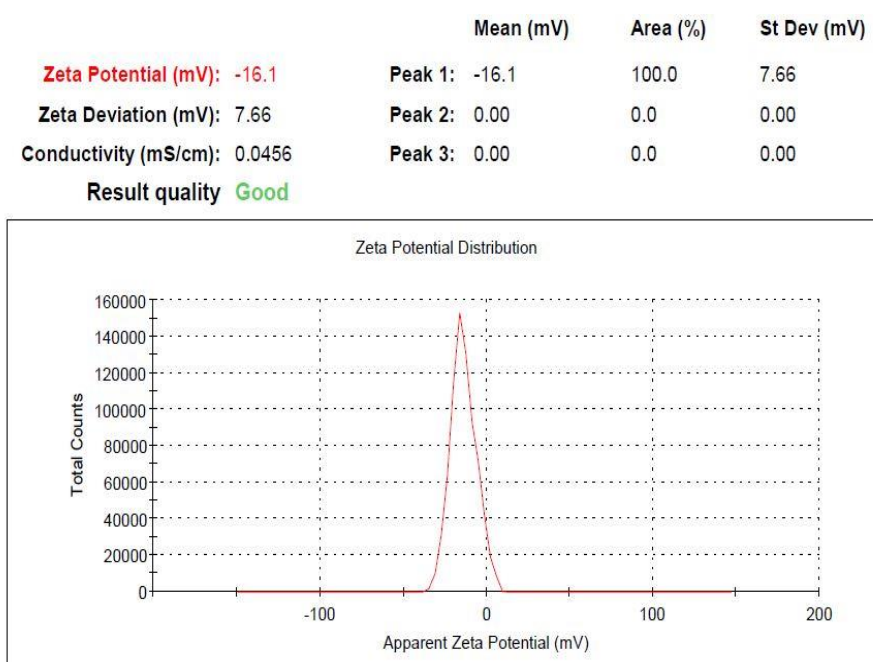
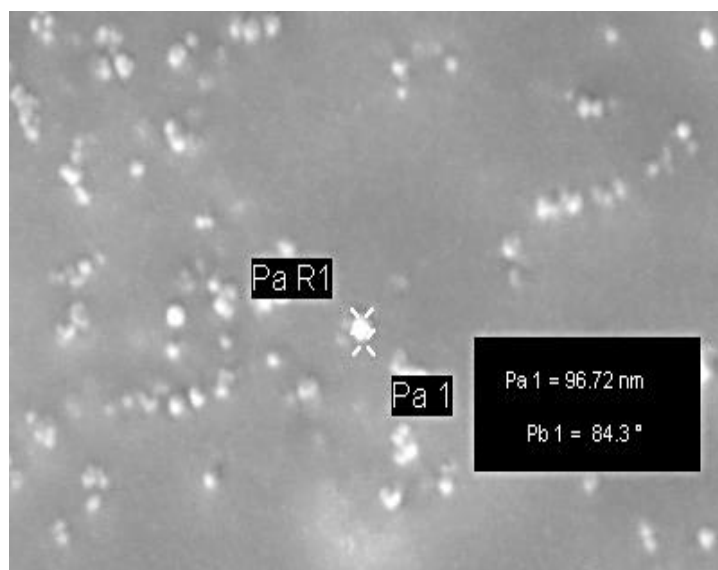


Figure 5A.18 Zeta potential of the developed Omiganan nano-lipid constructs



Scale of 2 μm

Figure 5A.19 SEM image of the developed Omiganan loaded nano-lipid constructs

	Size (d.nm):	% Intensity:	St Dev (d.nm):
Z-Average (d.nm): 115.7	Peak 1: 126.5	100.0	42.23
Pdl: 0.125	Peak 2: 0.000	0.0	0.000
Intercept: 0.949	Peak 3: 0.000	0.0	0.000
Result quality: Good			

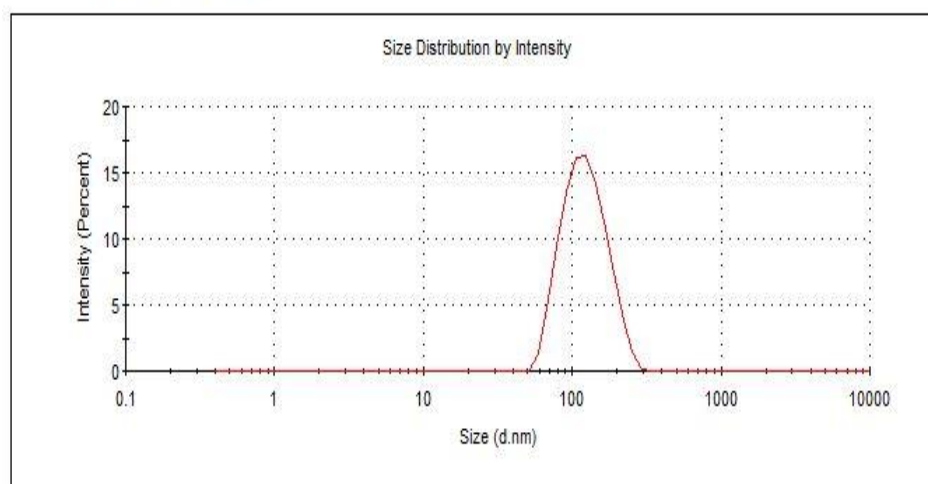


Figure 5A.20 Particle size of the optimized Omiganan nano-lipid constructs

5A.4.2.3 % Drug entrapment and % drug loading

% Drug entrapment and % drug loading of the optimized Omiganan NLCs were found to be 79.49 ± 1.26 % and 12.7 ± 0.5 % w/w, respectively.

5A.4.2.4 Viscosity of Omiganan NLC gel

The viscosity of free Omiganan gel and Omiganan NLC gel was found to be 12.49 ± 0.367 Pa.S and 15.42 ± 0.37 Pa.S, respectively. The increase in viscosity of NLC gel as compared to free Omiganan gel further leads to higher retention of NLC gel on the skin.

5A.4.2.5 Spreadability of Omiganan NLC gel

The spreadability of free Omiganan gel and Omiganan NLC gel was found to be 6.21 ± 2.34 cm² and 8.32 ± 1.85 cm², respectively, demonstrates the good spreadability of the formulated gel. The spreadability of free Omiganan gel was lesser than Omiganan NLC gel which may be attributed to the increased solid content of the gel after the addition of NLC formulation.

5A.4.2.6 pH of Omiganan NLC gel

The pH of free Omiganan gel and Omiganan NLC gel was found to be 6.4 ± 0.3 and 6.6 ± 0.3 , respectively, clearly resembles the pH of the skin thereby preventing irritation.

5A.4.2.7 Assay of Omiganan gel

The Omiganan content in free Omiganan gel and Omiganan NLC gel was found to be 99.20 ± 1.10 % and 98.77 ± 1.49 %, respectively.

5A.5 References

1. Sharma, G., et al., *Nanostructured lipid carriers: a new paradigm in topical delivery for dermal and transdermal applications*. Critical Reviews™ in Therapeutic Drug Carrier Systems, 2017. **34**(4).
2. Souto, E.B., et al., *SLN and NLC for topical, dermal, and transdermal drug delivery*. Expert opinion on drug delivery, 2020. **17**(3): p. 357-377.
3. Garcês, A., et al., *Formulations based on solid lipid nanoparticles (SLN) and nanostructured lipid carriers (NLC) for cutaneous use: A review*. European Journal of Pharmaceutical Sciences, 2018. **112**: p. 159-167.
4. Rehman, S., et al., *Tailoring lipid nanoconstructs for the oral delivery of paliperidone: Formulation, optimization and in vitro evaluation*. Chemistry and Physics of Lipids, 2021. **234**: p. 105005.

5. Carvajal-Vidal, P., et al., *Development of Halobetasol-loaded nanostructured lipid carrier for dermal administration: Optimization, physicochemical and biopharmaceutical behavior, and therapeutic efficacy*. *Nanomedicine: Nanotechnology, Biology and Medicine*, 2019. **20**: p. 102026.
6. Qumber, M., et al., *BBD-based development of itraconazole loaded nanostructured lipid carrier for topical delivery: in vitro evaluation and antimicrobial assessment*. *Journal of Pharmaceutical Innovation*, 2020: p. 1-14.
7. Rathod, V.R., D.A. Shah, and R.H. Dave, *Systematic implementation of quality-by-design (QbD) to develop NSAID-loaded nanostructured lipid carriers for ocular application: preformulation screening studies and statistical hybrid-design for optimization of variables*. *Drug development and industrial pharmacy*, 2020. **46**(3): p. 443-455.
8. Lawrence, X.Y., *Pharmaceutical quality by design: product and process development, understanding, and control*. *Pharmaceutical research*, 2008. **25**(4): p. 781-791.
9. Tarley, C.R.T., et al., *Chemometric tools in electroanalytical chemistry: methods for optimization based on factorial design and response surface methodology*. *Microchemical journal*, 2009. **92**(1): p. 58-67.
10. Ferreira, S.C., et al., *Box-Behnken design: an alternative for the optimization of analytical methods*. *Analytica chimica acta*, 2007. **597**(2): p. 179-186.
11. Mitra, S., et al., *Tumour targeted delivery of encapsulated dextran–doxorubicin conjugate using chitosan nanoparticles as carrier*. *Journal of Controlled Release*, 2001. **74**(1): p. 317-323.
12. Batheja, P., et al., *Topical drug delivery by a polymeric nanosphere gel: formulation optimization and in vitro and in vivo skin distribution studies*. *Journal of controlled release*, 2011. **149**(2): p. 159-167.
13. Shah, K.A., et al., *Solid lipid nanoparticles (SLN) of tretinoin: potential in topical delivery*. *International journal of pharmaceutics*, 2007. **345**(1-2): p. 163-171.
14. Kępczyński, M., et al., *Which physical and structural factors of liposome carriers control their drug-loading efficiency?* *Chemistry and physics of lipids*, 2008. **155**(1): p. 7-15.

15. Doppalapudi, S., et al., *Psoralen loaded liposomal nanocarriers for improved skin penetration and efficacy of topical PUVA in psoriasis*. European journal of pharmaceutical sciences, 2017. **96**: p. 515-529.
16. Chauhan, I., et al., *Nanostructured lipid carriers: A groundbreaking approach for transdermal drug delivery*. Advanced pharmaceutical bulletin, 2020. **10**(2): p. 150.
17. Hammond, K., et al., *Characterisation of phosphatidylcholine/phosphatidylinositol sonicated vesicles. Effects of phospholipid composition on vesicle size*. Biochimica et Biophysica Acta (BBA)-Biomembranes, 1984. **774**(1): p. 19-25.
18. Kumar, N. and S. Goindi, *Development, characterization and preclinical evaluation of nanosized liposomes of itraconazole for topical application: 32 full factorial design to estimate the relationship between formulation components*. Journal of Drug Delivery Science and Technology, 2021. **66**: p. 102785.
19. Qumber, M., et al., *BBD-based development of itraconazole loaded nanostructured lipid carrier for topical delivery: in vitro evaluation and antimicrobial assessment*. Journal of pharmaceutical innovation, 2021. **16**(1): p. 85-98.
20. Nagaich, U. and N. Gulati, *Nanostructured lipid carriers (NLC) based controlled release topical gel of clobetasol propionate: design and in vivo characterization*. Drug delivery and translational research, 2016. **6**(3): p. 289-298.